Numerical simulation of a direct current glow discharge in atmospheric pressure helium*

Zeng-Qian Yin(尹增谦)[1], Yan Wang(汪岩)[1,2], Pan-Pan Zhang(张盼盼)[2], Qi Zhang(张琦)[2], and Xue-Chen Li(李雪辰)[2,†]

[1] *Department of Mathematics and Physics, North China Electric Power University, Baoding* 071003, *China*
[2] *College of Physics Science & Technology, Hebei University, Baoding* 071002, *China*

(Received 5 July 2016; revised manuscript received 20 August 2016; published online 25 October 2016)

Characteristics of a direct current (DC) discharge in atmospheric pressure helium are numerically investigated based on a one-dimensional fluid model. The results indicate that the discharge does not reach its steady state till it takes a period of time. Moreover, the required time increases and the current density of the steady state decreases with increasing the gap width. Through analyzing the spatial distributions of the electron density, the ion density and the electric field at different discharge moments, it is found that the DC discharge starts with a Townsend regime, then transits to a glow regime. In addition, the discharge operates in a normal glow mode or an abnormal glow one under different parameters, such as the gap width, the ballast resistors, and the secondary electron emission coefficients, judged by its voltage–current characteristics.

Keywords: direct current discharge, one-dimensional fluid model, Townsend regime, glow regime

PACS: 52.65.−y, 52.80.Tn, 52.80.Hc **DOI:** 10.1088/1674-1056/25/12/125203

1. Introduction

Atmospheric pressure non-equilibrium plasma (APNP) has received increasing attention largely because of its low cost and simplified operation in comparison with low pressure discharge.[1] It has application prospects in a variety of fields, such as surface modification, ozone generation, biological sterilization and pollution control.[2–5] Streamer discharge is usually involved in APNP,[6] which is almost intrinsically inhomogeneous. As far as some special applications such as surface modification are concerned, it is more important to generate atmospheric pressure uniform discharge (APUD). According to the discharge mechanism, APUD can be categorized into atmospheric pressure glow discharge (APGD) and atmospheric pressure Townsend discharge (APTD).

Dielectric barrier discharge (DBD) is a traditional way of initiating APUD.[7,8] The DBD in helium has been originally reported by Kanazawa *et al.*[9] Since then, many investigations have been carried out in different kinds of working gases.[10–14] The evolution from APTD to APGD has been found experimentally within a discharge pulse by Lee *et al.*[10] According to a one-dimensional fluid model, Zhang and Kortshagen have found that it is APTD at a lower frequency but APGD at a higher frequency in a mixture of helium and oxygen.[11] The mode transition from APTD to APGD has also been numerically investigated by varying the external driving frequency in helium mixed with nitrogen.[12] Through numerical simulation, Wang *et al.* pointed out that APTD and APGD can be respectively obtained in atmospheric helium DBD under different frequencies.[13,14]

Compared with DBD, direct current (DC) discharge is one of the easy methods of generating APUD.[15] It has been realized in helium, argon, hydrogen, nitrogen, and air, moreover, and the discharge characteristics have been analyzed by the visualization of the discharges and the voltage–current curve.[16] A self-sustained glow discharge in atmospheric-pressure helium has been investigated experimentally.[17] Leys *et al.* have found that the DC discharge can also operate in APGD mode, which has similar characteristic regions to the low pressure glow discharge.[18,19] Deng *et al.* have pointed out that the DC discharge can be sustained in two different regimes: a self-pulsing regime at low current and a continuous glow regime at high current.[20] The transition from APTD to APGD has been investigated through two-dimensional numerical simulation on the DC discharge with moderate pd value, where p is gas pressure and d is the electrode spacing.[21] Recently, the APUD generated by a DC discharge with a semiconductor layer has been investigated numerically.[22]

Although APUDs have been investigated experimentally and numerically, it is still necessary to gain an in-depth insight into the influences of experimental parameters on the discharge mode in a steady state. Therefore, in this paper the APUD generated by the DC discharge is investigated in detail through one-dimensional fluid simulation.

2. Model description

The discharge initiates between two parallel–plate electrodes[23,24] as shown in Fig. 1. A DC voltage is applied

*Project supported by the National Natural Science Foundation of China (Grant Nos. 11575050 and 10805013), the Midwest Universities Comprehensive Strength Promotion Project, the Natural Science Foundation of Hebei Province, China (Grant Nos. A2016201042 and A2015201092), and the Research Foundation of Education Bureau of Hebei Province, China (Grant No. LJRC011).

†Corresponding author. E-mail: plasmalab@126.com

© 2016 Chinese Physical Society and IOP Publishing Ltd

across the two electrodes and a ballast resistor R is used to restrict the discharge current in order to obtain an APUD. The gas gap width (d_g) is filled with pure helium under atmospheric pressure.

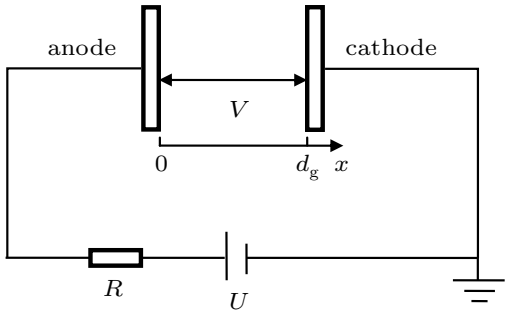


Fig. 1. Schematic diagram of the DC discharge.

Numerical simulation is based on a one-dimensional fluid model. Electrons and ions are described by the continuity equations:

$$\frac{\partial n_{e,p}}{\partial t} + \frac{\partial j_{e,p}}{\partial x} = S, \tag{1}$$

where n, j, and S are the charged particle number density, flux, and source function, respectively. Subscripts e and p represent the electron and ion, respectively. With the drift-diffusion approximation, the flux term is given by

$$j_{e,p} = \mp \mu_{e,p} n_{e,p} E - D_{e,p} \frac{\partial n_{e,p}}{\partial x}, \tag{2}$$

where E is the electric field, μ_e and μ_p are electron mobility and ion mobility, and D_e and D_p are diffusion coefficients of electron and ion, respectively.[25,26] In the source term, the direct ionization by electron impact and the recombination between electron and ion are considered. Therefore, the source term could be calculated from the following formula:

$$S = \alpha \mu_e |E| n_e - \beta n_e n_p, \tag{3}$$

where α is the Townsend ionization coefficient and β is the combination rate coefficient.[25,27] Instead of solving Poisson's equation, the electric field is given from the current conservation equation:[28]

$$\varepsilon(x) \frac{\partial E(x,t)}{\partial t} + i_C(x,t) = i_T(t), \tag{4}$$

where i_T, i_C, and ε_0 are the total current density, the conduction current density, and the permittivity of vacuum, respectively. i_C is given by

$$i_C(x,t) = e(j_p(x,t) - j_e(x,t)). \tag{5}$$

The secondary electron emission coefficient from the cathode (γ) is considered here for ion bombardment alone, and the electron flux leaving the cathode is taken as $\gamma j_p(x,t)$. The expression of $i_T(t)$ can be obtained by integrating Eq. (4) from $x = 0$ to $x = d_g$.:

$$i_T = \frac{\varepsilon_0}{d_g} \frac{\partial V}{\partial t} + \frac{1}{d_g} \int_0^{d_g} i_C(x,t)\,\mathrm{d}x, \tag{6}$$

where V is the gas voltage between the two electrodes. The external circuit equation can be written as

$$U = V + i_T R, \tag{7}$$

where U is the applied voltage.

A set of equations listed above is solved by the Scharfetter–Gummel scheme.[29] The simulation parameters are chosen as follows. The gas temperature is set to be 300 K in atmospheric pressure helium. Initial densities of electrons and ions in the gas gap are considered to be uniform with $n_e(x,0) = n_p(x,0) = 10^7$ cm^{-3}.

3. Results and discussion

In the simulation, the electron–ion recombination rate coefficient β and the electron diffusion coefficients D_e are needed. They are calculated from the formula

$$\beta = 8.1 \times 10^{-20} \frac{n_e}{1 + 0.079p} \left(\frac{T_e}{T_g}\right)^{-4.4} \quad \text{and} \quad D_e = \frac{kT_e\mu_e}{|q|},$$

respectively. Under constant peak voltage ($U = 3$ kV) and ballast resistor ($R = 100$ kΩ), figure 2(a) shows the temporal evolutions of current density at different electron temperatures.

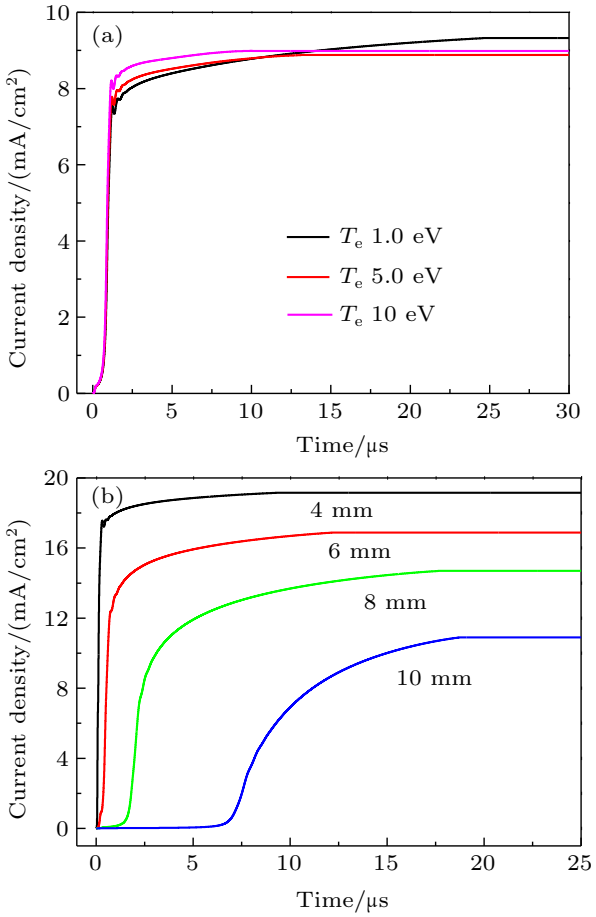


Fig. 2. (color online) Temporal evolutions of the current density at different electron temperatures (a), and under different gap widths (b). Other parameters: $U = 3$ kV and $R = 100$ kΩ.

It can be found that the discharge does not reach its steady state till it takes a period of time. Moreover, the required time decreases with increasing the electron temperature. It can also be found that T_e has a slight influence on the current density of the steady state. Therefore, T_e is selected as a constant (1.5 eV) in the following simulation. Figure 2(b) shows the temporal evolutions of current density under different gap widths. It can be found from Fig. 2(b) that the required time increases and the current density of the steady state decreases with increasing the gap width.

Figure 3 presents the spatial distributions of electron density, ion density and the electric field at the moments of 0.3 μs, 0.9 μs, 3 μs, and 20 μs, respectively. The electric field is almost uniformly distributed along the gap and the density maxima for electron and ion appear near the anode at the beginning of the discharge as shown in Fig. 3(a). In the Townsend regime, the electron avalanches develop from the cathode to the anode and the densities for electron and ion increase in the process. Hence, the maxima of both electron density and ion density appear near the anode. Therefore, it can be concluded that the discharge belongs to APTD at the beginning. Comparing Fig. 3(a) with Fig. 3(b), it can be found that the maxima of electron density and ion density shift toward the cathode with time elapsing. At the moment of 3 μs, a cathode fall region can be discerned in Fig. 3(c). In the cathode fall region, it is clear that the electric field near the cathode increases almost linearly along the x axis, which is very similar to that observed in a low-pressure glow discharge.[30] This result also accords with the field profile measured spectroscopically for a helium DC atmospheric pressure glow discharge.[17] Therefore, the existence of the cathode fall region verifies that the discharge operates in a glow discharge mode. Figure 3(d) shows the spatial distributions of electron density, ion density and the electric field corresponding to the steady discharge state. Obviously, there is an anode region near the anode, which is followed by a positive column, and a cathode fall region near the cathode. In the positive column, the electric field is lower than that in the anode region or the cathode fall region. Therefore, it can be concluded that the discharge has a transition from the APTD to APGD in the discharge process.

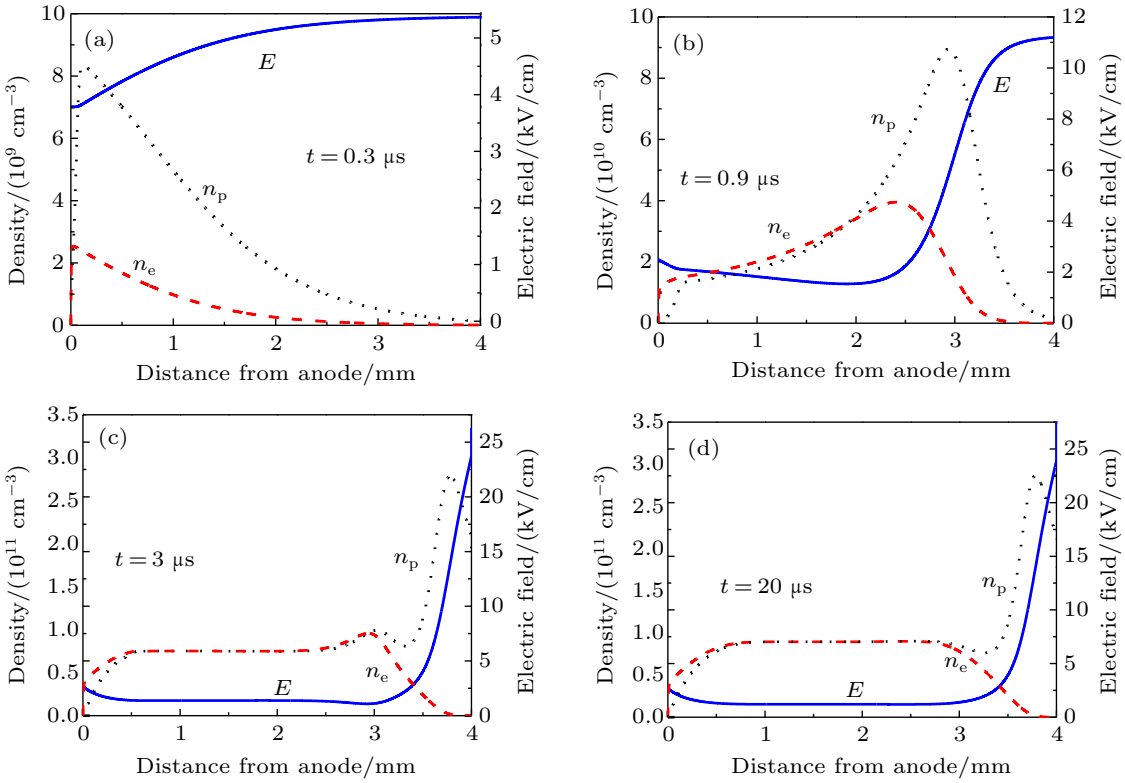


Fig. 3. (color online) Spatial distributions of the electron density, the ion density, and the electric field at different times: (a) 0.3 μs, (b) 0.9 μs, (c) 3.0 μs, and (d) 20.0 μs. Other parameters: $d_g = 4$ mm, $U = 3$ kV, and $R = 100$ kΩ.

In order to have a better understanding about the DC discharge mode, the discharge voltage–current (V–I) curves in a steady state are investigated for different parameters. Figure 4 presents the V–I curves for the DC discharge under different gap widths. With increasing i_T, gas voltage increases monotonically for a wider gap, such as $d_g = 10$ mm and $d_g = 4$ mm, and it decreases monotonically for a narrower gap ($d_g = 2$ mm). The positive slope of the V–I curve is an indication that the discharge operates in the abnormal glow mode. At the same time, the negative slope indicates that the discharge is in the normal glow mode. It has been originally found in the glow discharge at low pressure.[16] Recently, it has also been verified in an atmospheric pressure glow discharge.[22] Therefore, it can be concluded that the discharge operates in the ab-

normal glow mode for a wider gap and the normal glow mode for a narrower gap. As is well known, an electron avalanche quickly builds up in the gas gap. Apparently, it tends to grow into a bigger avalanche with a wider gap if other parameters remain constant. The bigger the avalanche, the higher the obtained current density will be, which means that the discharge tends to operate in the abnormal glow mode. Therefore, the discharges operate in the normal glow mode for the narrower gap and the abnormal glow mode for the wider gap, respectively.

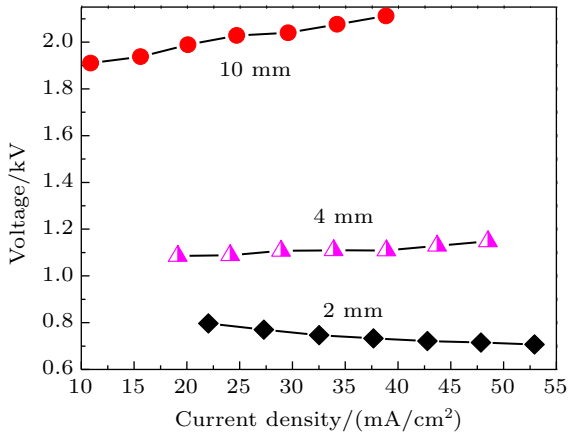


Fig. 4. (color online) Voltage–current curves for the atmospheric pressure discharge under different gap widths. The ballast resistor is 100 kΩ.

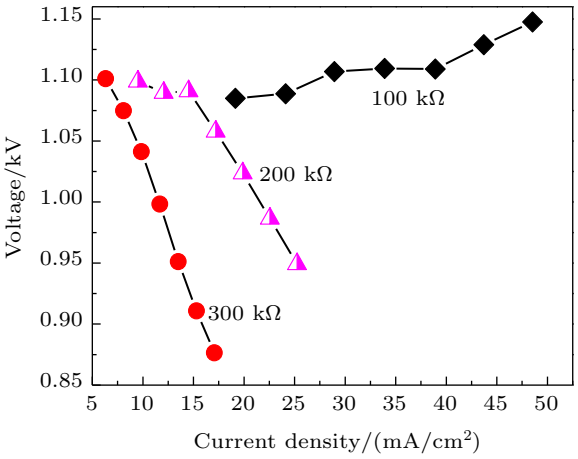


Fig. 5. (color online) Voltage–current curves with different ballast resistors. The gap width is 4.0 mm for the atmospheric pressure helium.

Figure 5 shows the V–I curves with different ballast resistors for $d_g = 4$ mm. It can be found that with increasing i_T, the V increases monotonically for a small resistor ($R = 100$ kΩ), decreases monotonically for a large resistor ($R = 300$ kΩ) and maintains almost a constant at lower current density and then decreases monotonically for $R = 200$ kΩ. It can be concluded that the discharges operate in the abnormal glow mode for a smaller resistor and in the normal glow mode for a larger resistor, respectively. As mentioned above, the resistor is used to restrict the increase of the discharge current. Therefore, the discharge current will be maintained at a lower value for a larger resistor, which means that the discharge tends to stay in a normal glow mode for a larger resistor. Consequently, the discharges operate in the abnormal glow mode for a smaller resistor and in the normal glow mode for a larger resistor, respectively.

Figure 6 displays the V–I curves with different secondary electron emission coefficients for $d_g = 4$ mm and $R = 100$ kΩ. Apparently, with increasing i_T, the gas voltage increases monotonically for different values of secondary electron emission coefficient. It can also be seen that the lower secondary electron emission coefficient corresponds to the larger voltage for the same current density. The positive slope of the V–I curve is an indication that the discharge operates in the abnormal glow mode, which means that a small variance of the secondary electron emission coefficient does not affect the discharge mode.

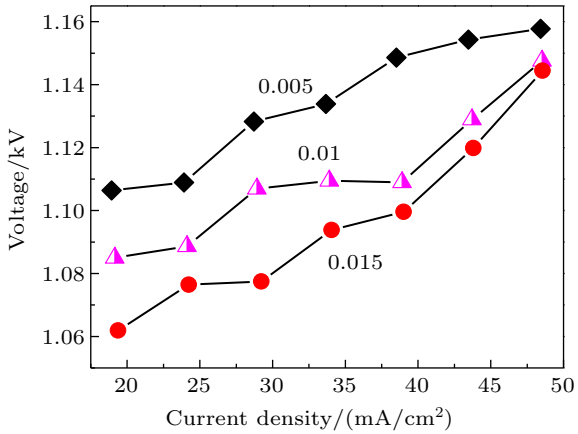


Fig. 6. (color online) Voltage–current curves with different coefficients for the secondary electron emission. Other parameters: $d_g = 4$ mm and $R = 100$ kΩ.

4. Conclusions

Based on a one-dimensional fluid model, the characteristics of DC discharge in atmospheric pressure helium are investigated. Results indicate that the discharge does not reach its steady state till it takes a period of time. Moreover, the required time increases and the current density of the steady state decreases with increasing the gap width. Through analyzing the spatial distributions of the electron density, the ion density and the electric field at different discharge moments, it is found that the DC discharge starts with the Townsend regime, then transits to the glow regime. In addition, the discharge operates in a normal glow mode or an abnormal glow one under different parameters, such as the gap width, the ballast resistors, and the secondary electron emission coefficients, judged by its voltage–current characteristics. The discharge operates in a normal glow mode, a narrower gas gap and larger ballast resistor. For a wider gap or smaller resistor, the discharge operates in an abnormal glow mode. It is also found that the discharge always operates in an abnormal glow mode with a small variance of the secondary electron emission coefficient.

References

[1] Sun W, Li G and Li H 2007 *Appl. Phys. Lett.* **101** 123302

[2] Zhang Z, Qiu Y and Lou Y 2003 *J. Phys. D: Appl. Phys.* **36** 2980
[3] Deng X T and Shi J J 2005 *Appl. Phys. Lett.* **87** 153901
[4] Plaksin V Y, Penkov O V, Ko M K and Lee H J 2010 *Plasma Sci. Technol.* **12** 688
[5] Lu X, Naidis G V, Laroussi M, Reuter S, Graves D B and Ostrikov K 2016 *Phys. Rep.* **630** 1
[6] Lu X, Naidis G V, Laroussi M and Ostrikov K 2014 *Phys. Rep.* **540** 123
[7] Fang Z, Qiu Y, Zhang C and Kuffel E 2007 *Plasma Sources Sci. Technol.* **40** 1401
[8] Yang D, Li S, Nie D, Zhang S and Wang W 2012 *Plasma Sources Sci. Technol.* **21** 035004
[9] Kanazawa S, Kogoma M and Moriwaki T 1988 *J. Phys. D: Appl. Phys.* **21** 838
[10] Lee D, Park J M, Hong S H and Kim Y 2005 *IEEE Trans. Plasma Sci.* **33** 949
[11] Zhang P and Kortshagen U 2006 *J. Phys. D: Appl. Phys.* **39** 153
[12] Luo H Y, Liang Z, Lv B, Wang X X, Guan Z C and Wang L M 2007 *Appl. Phys. Lett.* **91** 221504
[13] Wang Q, Sun J Z and Wang D Z 2009 *Phys. Plasmas* **16** 043503
[14] Wang Q, Sun J Z and Wang D Z 2011 *Phys. Plasmas* **18** 103504
[15] Akishev Y S, Goossens O, Callebaut T, Leys C, Napartovich A and Trushkin N 2001 *J. Phys. D: Appl. Phys.* **34** 2875
[16] Raizer Y P 1991 *Gas Discharge Physics* (Berlin: Springer-Verlag)
[17] Arkhipenko V I, Zgirovskii S M, Kirillov A A and Simonchick L V 2002 *Plasma Phys. Rep.* **28** 858
[18] Leys C, Bruggeman P, Liu J J, Degroote J, Kong M G and Vierendeels J 2008 *J. Phys. D: Appl. Phys.* **41** 215201
[19] Leys C and Bruggeman P 2009 *J. Phys. D: Appl. Phys.* **42** 053001
[20] Deng X L, Nikiforov A Y, Vanraes P and Leys C 2013 *J. Appl. Phys.* **113** 023305
[21] Robert R A and Vladimir I K 2003 *J. Phys. D: Appl. Phys.* **36** 2986
[22] Liu F C, Yan W and Wang D Z 2013 *Phys. Plasmas* **20** 122116
[23] Li X C, Niu D Y, Yin Z Q, Fang T Z and Wang L 2012 *Phys. Plasmas* **19** 083505
[24] Li X C, Niu D Y, Xu L F, Jia P Y and Chang Y Y 2012 *Chin. Phys. B* **21** 075204
[25] Deloche R, Monchicourt P and Cheret M, *et al.* 1976 *Phys. Rev. A* **13** 1140
[26] Xu X J 1996 *Discharge Physics of Gas* (Shanghai: Fudan University Press) p. 277
[27] Ward A L 1962 *J. Appl. Phys.* **33** 2789
[28] Kulikovsky AA 1994 *J. Phys. D: Appl. Phys.* **27** 2556
[29] Scharferter D L and Gummel H K 1969 *IEEE Trans. Electron. Dev.* **16** 64
[30] Davies A J and Evans J G 1980 *J. Phys. D: Appl. Phys.* **13** 161